Cocrystals of nutraceutical *p*-coumaric acid with caffeine and theophylline: polymorphism and solid-state stability explored in detail using their crystal graphs†

Nate Schultheiss*, Melanie Roe and Stephan X. M. Boerrigter

Received 18th May 2010, Accepted 14th August 2010
DOI: 10.1039/c0ce00214c

Cocrystals constructed with *p*-coumaric acid (a phytochemical and nutraceutical compound) are investigated with xanthine compounds, caffeine and theophylline. Four cocrystals of *p*-coumaric acid with caffeine (1 : 1 and 1 : 2 stoichiometric ratios) and theophylline (two 1 : 1 polymorphs, Form I and Form II) were generated and their structures determined by single-crystal X-ray crystallography. The two theophylline cocrystals display synthon polymorphism, where both structures possess a carboxylic acid–imidazole heteromeric synthon; however, one polymorph also has a hydroxyl–carbonyl synthon (Form I), while in the other a hydroxyl–imidazole synthon (Form II) is present. Furthermore, the solid-state stability of the two *p*-coumaric acid : theophylline polymorphs was explored experimentally and computationally.

Introduction

Cocrystals are multi-component crystals in which the individual, neutral molecules are held together by non-covalent interactions, most often hydrogen bonds.[1] Cocrystalline materials containing active pharmaceutical ingredients (APIs) are continuing to gain interest within the pharmaceutical industry, due to their ability to alter the physicochemical properties of solid dosage forms, while providing additional opportunities for intellectual property and drug product repositioning.[2] Generating cocrystals of an API can be advantageous because (1) it allows for modifications to be introduced to the crystal structure of a drug (which in turn can alter its physical and chemical properties) without compromising its intended bioactivity, and (2) it gives rise to the possibility of generating combination drugs where two or more active ingredients are brought into one crystal lattice.

When engineering a cocrystal, major criteria for selecting a cocrystal former (coformer), especially if the cocrystal is intended as a final drug product, are its pharmacological and toxicological properties. A number of different sources are often used for selecting a suitable coformer, including the pharmaceutically acceptable salt formers list,[3] Generally Regarded as Safe (GRAS) list,[4] and Everything Added to Food in the United States (EAFUS) list.[5] In addition to the possible coformers on these lists, formulation excipients,[6] as well as complementary drug molecules and nutraceutical compounds[7] (resulting in possible combination drugs)[8] could also be potentially incorporated into the construction of a cocrystal.

Coumaric acid is a hydroxy derivative of cinnamic acid and naturally occurs in three isomers (*ortho*-, *meta*-, and *para*-); *p*-coumaric acid is the most commonly occurring isomer in nature. Classified as a phytochemical and nutraceutical, *p*-coumaric acid is found in various edible plants, such as peanuts, carrots, and tomatoes.[9] A number of promising pharmacokinetic studies have been conducted on *p*-coumaric acid showing a positive response in protection against colon cancer on cultured mammalian cells,[10] as well as antioxidant and anti-inflammatory properties in rats and rabbits.[11] Caffeine and theophylline are both classified as xanthine alkaloids, with the former often used as a food additive and central nervous system stimulant, while the latter has shown health benefits in the treatment of asthma.[12]

Herein we report the synthesis and characterization of four cocrystals of *p*-coumaric acid with caffeine and theophylline, including single crystal X-ray structure determination for each. Additionally, the solid-state stability of the two polymorphic *p*-coumaric acid : theophylline cocrystals is examined in-depth, in particular how the synthons relate to the intermolecular interaction energies. The chemical structures of the compounds used in this study are shown in Scheme 1.

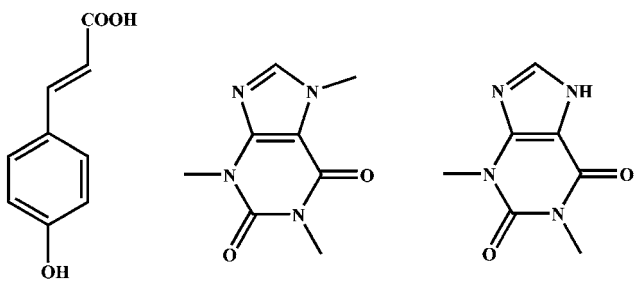

Scheme 1 Chemical structures of *p*-coumaric acid, caffeine, and theophylline (L–R).

SSCI, a Division of Aptuit, 3065 Kent Avenue, West Lafayette, IN, 47906, USA. E-mail: Nathan.schultheiss@aptuit.com; Fax: +1-765-463-4722; Tel: +1-765-463-0112

† Electronic supplementary information (ESI) available: XRPD patterns, DSC and TGA thermograms of **1–4**, and COMPASS calculations. CCDC reference numbers 778271–778272. For ESI and crystallographic data in CIF or other electronic format see DOI: 10.1039/c0ce00214c.

Experimental

Reagents

p-Coumaric acid, caffeine, and theophylline (anhydrous) were purchased from Sigma-Aldrich and used as received. All other chemicals were purchased from various suppliers and used without further purification.

p-Coumaric acid : caffeine (1 : 1), 1

Single crystals were grown from a slow cool experiment where a 1 : 1 mixture of *p*-coumaric acid (57.3 mg, 0.35 mmol) and caffeine (67.7 mg, 0.35 mmol) was dissolved in acetonitrile (3.8 mL) with stirring at approximately 70 °C. Upon cooling to room temperature and standing for 1 day, single crystals were harvested. The material was scaled up following the same reaction procedure resulting in 702 mg, 80% yield.

p-Coumaric acid : caffeine (1 : 2), 2

Single crystals were grown from a slow evaporation experiment. A bulk solution of *p*-coumaric acid (194.0 mg, 1.18 mmol) in acetone (4.0 mL) was initially prepared. A small amount of this solution (600 μL, containing 0.18 mmol *p*-coumaric acid) was added to a vial, and a solution of caffeine (35.7 mg, 0.18 mmol) in acetone (5.0 mL) was added with stirring. The solution was allowed to slowly evaporate, upon which single crystals were culled. The material was scaled up following the same reaction procedure resulting in 1.03 g, 64% yield. No attempt was made to improve the yield by reacting the components in a 1 : 2 stoichiometric ratio.

p-Coumaric acid : theophylline (1 : 1), 3 (Form 1) and 4 (Form II)

Single crystals were grown from a slow evaporation experiment. A bulk solution of *p*-coumaric acid (194.0 mg, 1.18 mmol) in acetone (4.0 mL) was initially prepared. A small amount of this solution (600 μL, containing 0.18 mmol *p*-coumaric acid) was added to a vial, and a solution of theophylline (32.7 mg, 0.18 mmol) in methanol (5.0 mL) was added with stirring in a 1 : 1 molar ratio. The solution was allowed to slowly evaporate, upon which single crystals of **3** and **4** were culled. Larger quantities of pure **3** (Form I) and **4** (Form II) were generated by adding solid theophylline to a nearly saturated solution of *p*-coumaric acid in ethanol for (Form I) or *p*-dioxane for (Form II) and stirring for ~24 hours before filtering.

Interconversion slurries

Saturated solutions of *p*-coumaric acid and theophylline were prepared by adding solids of each component to three different solvents (acetonitrile, ethyl acetate, and isopropanol) until undissolved solids were present. Equal amounts (approximately 5 mg) of each *p*-coumaric acid : theophylline cocrystal, **3** (Form I) and **4** (Form II), were then added to a filtered portion of the liquid phase from each saturated solution, and the resulting slurries were allowed to stir at ambient conditions for 1 day. Solids were collected by vacuum filtration and analyzed by XRPD.

X-Ray powder diffraction (XRPD)

Patterns were collected using a PANalytical X'Pert Pro diffractometer. An incident beam of Cu Kα radiation was produced using an Optix long, fine-focus source. PANalytical data were collected and analysed using X'Pert Pro Data Collector software (v. 2.2b). Prior to the analysis, a silicon specimen (NIST SRM 640c) was analyzed to verify the Si 111 peak position. PANalytical diffraction patterns were collected using a scanning position-sensitive detector (X'Celerator) located 240 mm from the specimen.

Thermogravimetric analysis (TGA)

Thermogravimetric analyses were performed using a TA Instruments 2950 thermogravimetric analyzer. The sample was placed in an aluminium sample pan and inserted into the TG furnace. Analyses began at ~20 °C, and the furnace was heated under nitrogen at a rate of 5 or 10 K min^{-1}, up to a final temperature of 350 °C. Nickel and Alumel™ were used as calibration standards.

Differential scanning calorimetry (DSC)

DSC was performed using a TA Instruments 2920 differential scanning calorimeter. Temperature calibration was performed using NIST traceable indium metal. The sample was placed into an aluminium DSC pan, and the weight was accurately recorded. The pan was covered with a lid perforated with a laser pinhole, and the lid was crimped. A weighed, crimped aluminium pan was placed on the reference side of the cell. The sample cell was equilibrated at 25 °C and heated under a nitrogen purge at a rate of 5 or 10 K min^{-1}, up to a final temperature of 250 °C.

Single crystal X-ray diffraction (SCXRD)

Datasets were collected on a Bruker SMART APEX II diffractometer (**1**, **2** and **4**) or a Bruker Kappa APEX II diffractometer (**3**) using Mo Kα radiation. Data were collected using APEX II software.[13] Initial cell constants were found by small widely separated "matrix" runs. Data collection strategies were determined using COSMO. Scan speed and scan width were chosen based on scattering power and peak rocking curves. Temperature control was provided with an Oxford Cryostream low-temperature device.

Unit cell constants and orientation matrix were improved by least-squares refinement of reflections thresholded from the entire dataset. Integration was performed with SAINT,[14] using this improved unit cell as a starting point. Precise unit cell constants were calculated in SAINT from the final merged dataset. Lorenz and polarization corrections were applied. Absorption corrections were not applied ($\mu \times d < 0.05$ in all cases).

Data were reduced with SHELXTL.[15] The structures were solved in all cases by direct methods without incident. Unless otherwise noted, coordinates of all –OH and –NH hydrogens were refined. All other hydrogens were riding in idealized positions. Unless otherwise noted, all non-hydrogen atoms were refined using anisotropic thermal parameters. Refinement details for each cocrystal **1–4** are listed below.

1 Coordinates for the acid hydrogen atom H29, and the phenol hydrogen atom H24 were refined.

2 One of the two unique caffeines existed in two different orientations. The ratio for the two orientations was refined. A water of hydration was located in the difference Fourier map. Its occupancy and isotropic thermal parameter were refined; because of the low occupancy, hydrogen atoms for this water molecule were neither located nor included. Coordinates for the acid hydrogen atom H29, and the phenol hydrogen atom H24 were refined.

3 There were two independent acid : theophylline pairs in the asymmetric unit. Each pair was included in a SHELXL "RESI" residue. Coordinates for the two acid hydrogen atoms, both labelled H29, and both phenol hydrogen atoms H24 were refined.

4 Coordinates of amine hydrogen atom H17, phenol hydrogen atom H24, and carboxylic acid hydrogen atom H29 were all refined.

Molecular modelling

Crystal structures as obtained from SCXRD were imported into Materials Studio 5.0.0.0 (Accelrys Software Inc., San Diego) and appropriate bond orders were assigned. Full unit cell geometry optimizations were performed using the COMPASS 2.7 force field[16] using the force field's charge parameters. Lattice energies are reported as the final energies including all intra-molecular interaction energy contributions. Molecular interaction energies were calculated using all default settings using the "crystal graph" method as implemented in the morphology module. For the purpose of clarity in this presentation, only the interactions stronger than −2.0 kcal mol^{-1} are shown. The full set of interactions up to the default cut-off of −0.596 kcal mol^{-1} are tabulated in the ESI†.

AM1 calculations

Molecular structures were constructed using Spartan '08 (Wavefunction, Inc. Irvine, CA), and their geometries were optimized using AM1, with the maxima and minima in the electrostatic potential surface (0.002 e au^{-1} isosurface) determined using a positive point charge in vacuum as a probe.

Results and discussion

In efforts to generate cocrystals with *p*-coumaric acid and caffeine, two crystal structures with different stoichiometries were obtained. Cocrystal **1** was synthesized from slow cooling a 1 : 1 mixture of components, resulting in crystals with the monoclinic space group $P2_1/c$, Table 1. The asymmetric unit of **1** contains *p*-coumaric acid and caffeine in a 1 : 1 stoichiometric ratio, Fig. 1. In the crystal structure of **1**, the molecules assemble into one-dimensional chains through a series of heteromeric O–H···N, C–H···O and O–H···O hydrogen bonds. The carboxylic acid moiety of *p*-coumaric acid forms hydrogen bonds with the imidazole of caffeine through an $R_2^2(7)$ heterosynthon, while the hydroxyl moiety hydrogen bonds with the carbonyl oxygen of caffeine (O24···O16, 2.6984 Å), Fig. 2 and Table 2.

The second structure, cocrystal **2**, crystallizes in the triclinic space group $P\bar{1}$, Table 1. Although the crystals were formed from a 1 : 1 mixture of components in acetone, the asymmetric unit of **2** contains one molecule of *p*-coumaric acid and two molecules of

Table 1 Crystallographic data for **1–4**

	1	**2**	**3** (Form I)	**4** (Form II)
Empirical formula	$C_{17}H_{18}N_4O_5$	$C_{25}H_{28}N_8O_{7.20}$	$C_{16}H_{16}N_4O_5$	$C_{16}H_{16}N_4O_5$
M_w	358.35	555.75	344.33	344.33
Color, habit	Colorless, prism	Colorless, prism	Colorless, plate	Colorless, plate
Crystal size/mm^3	0.35 × 0.25 × 0.15	0.24 × 0.20 × 0.16	0.22 × 0.14 × 0.08	0.36 × 0.20 × 0.08
Crystal system	Monoclinic	Triclinic	Triclinic	Monoclinic
Space group, Z	$P2(1)/c$, 4	$P\bar{1}$, 2	$P\bar{1}$, 4	$P2(1)/n$, 4
a/Å	6.5225(4)	8.1475(7)	7.7073(6)	6.9196(11)
b/Å	10.6474(6)	11.2176(9)	14.2718(10)	26.801(4)
c/Å	23.2444(14)	14.8517(13)	14.7035(10)	8.6984(12)
α/°	90	75.956(2)	74.327(4)	90
β/°	93.983(2)	84.712(2)	82.294(5)	108.027(6)
γ/°	90	73.340(2)	83.154(5)	90
Volume/Å^3	1610.37(17)	1261.16(18)	1542.28(19)	1542.28(19)
Density/g cm^{-3}	1.478	1.464	1.483	1.491
Temperature/K	120(2)	120(2)	120(2)	120(2)
X-Ray wavelength	0.71073	1.54178	0.71073	0.71073
μ/mm^{-1}	0.111	0.110	0.113	0.113
$F(000)$	752	583	720	720
Θ_{min}/°	3.13	1.95	1.44	2.58
Θ_{max}/°	32.14	32.59	31.50	31.00
Reflections				
Collected	18 365	26 213	35 014	15 724
Independent	5512	8113	10 196	4826
Observed	4533	6433	5212	2868
R_{sigma}	0.025	0.026	0.086	0.0935
R_{int}	0.024	0.023	0.086	0.0838
Threshold expression	$>2\sigma(I)$	$>2\sigma(I)$	$>2\sigma(I)$	$>2\sigma(I)$
R_1 (observed)	0.0447	0.0538	0.0665	0.0955
wR_2 (all)	0.1367	0.1512	0.1793	0.2906

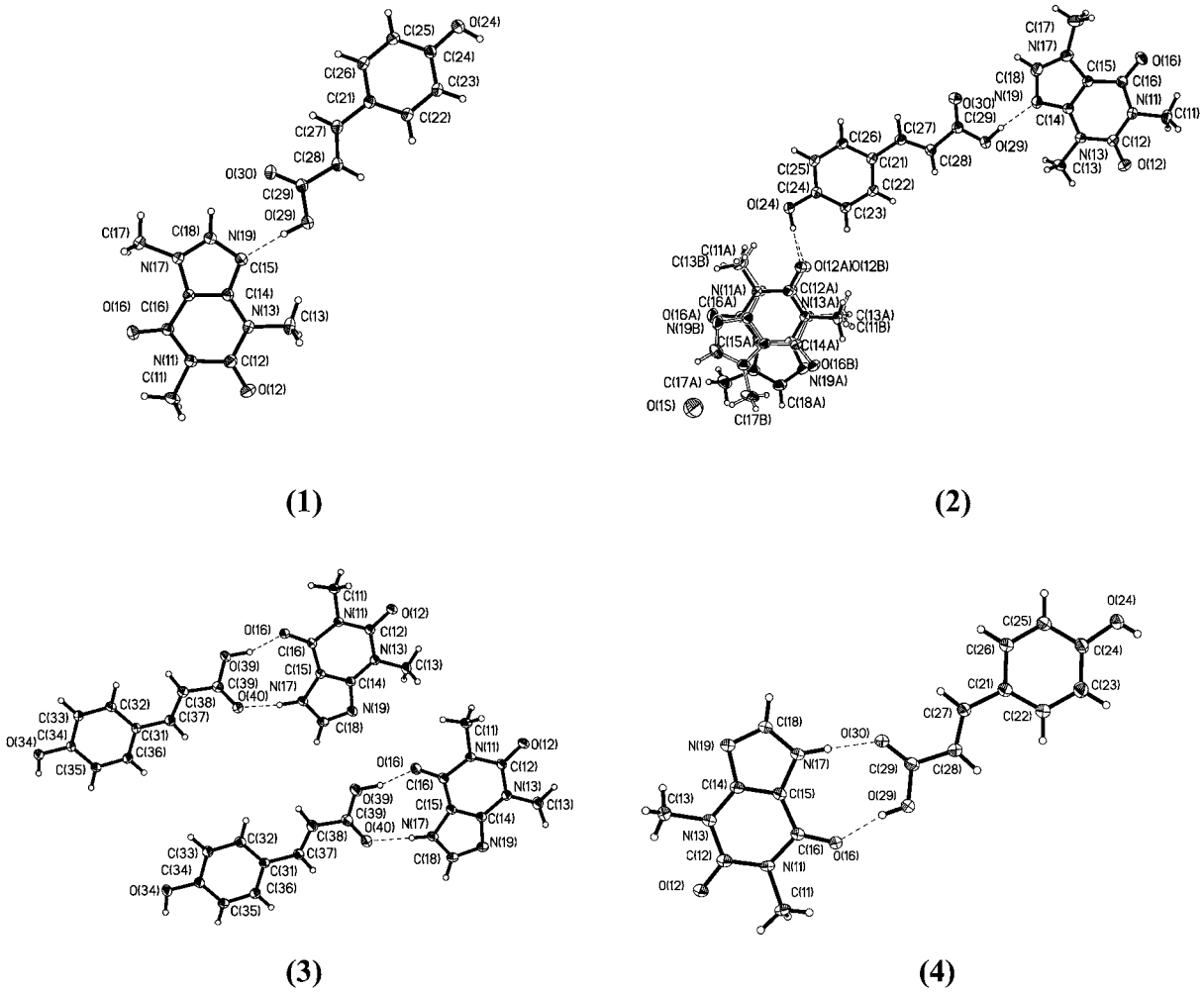

Fig. 1 Thermal ellipsoid plots and labelling schemes for **1–4**. Thermal ellipsoids are displayed at 50% probability level.

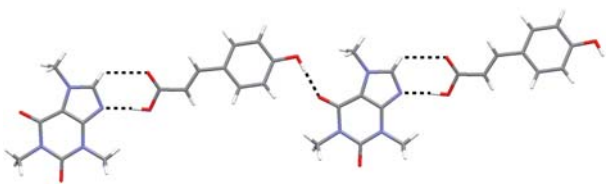

Fig. 2 Periodic one-dimensional chain formed through carboxylic acid–imidazole and hydroxyl–carbonyl heteromeric synthons in **1**.[17]

caffeine, Fig. 1. In the crystal structure of **2**, a discrete three-component supramolecular assembly is generated (Fig. 3) in contrast to the 1 : 1 one-dimensional chain formed in **1**. Once again, the carboxylic acid moiety of *p*-coumaric acid forms an O–H···N (O29–N19, 2.7129 Å) hydrogen bond with the imidazole nitrogen atom of caffeine, while the hydroxyl moiety forms an O–H···O (O24–O12A, 2.679 Å or O24–O12B, 2.719 Å) hydrogen bond with the carbonyl group of the second caffeine molecule. To be noted, the self-complementary C–H···O hydrogen bond from the imidazole of caffeine to the carbonyl of *p*-coumaric acid does not form even though the two molecules lie coplanar to one another. The C–H···O distance is 3.07 Å, which is well beyond the van der Waals distance for a hydrogen and oxygen contact, 2.72 Å. The refinement of the disorder of the caffeine molecule linked through the hydroxyl moiety resulted in site occupancies of 0.628 : 0.372. Additionally, the water molecule within the structure was assigned an occupancy of 0.20.

Interestingly, a 2 : 1 crystal structure between caffeine and 4-hydroxybenzoic acid (a structural analogue of *p*-coumaric acid) was recently reported, and it too displayed disorder around one caffeine molecule, resulting also in a discrete three-component assembly.[18]

Two polymorphic 1 : 1 *p*-coumaric acid : theophylline cocrystals resulted from a 10 : 1 methanol/acetone slow evaporation experiment. Cocrystal **3** (Form I) crystallizes in the triclinic space group $P\bar{1}$ (Table 1) with two independent 1 : 1 cocrystals of *p*-coumaric acid and theophylline in the asymmetric unit (due to structural similarity only one will be described), Fig. 1. The molecules are linked through heteromeric, self-complementary N–H···O and O–H···O hydrogen bonds from the carboxylic acid moiety to the imidazole hydrogen (N17···O41, 2.792 Å) and carbonyl moiety of the theophylline molecule (O39···O16, 2.618 Å). As observed in structure **1**, one-dimensional hydrogen bonded chains are formed through the hydroxyl moiety of *p*-coumaric acid to the carbonyl of theophylline (O34···O12#1, 2.721 Å). The one-dimensional rows are further linked into

Table 2 Hydrogen-bond geometries for **1–4**

Cocrystal	D–H···A	D(D–H)	d(H···A)	d(D···A)	<(DHA)
1	O(29)–H(29)···N(19)	0.925(16)	1.783(16)	2.7021(12)	172.3(15)
	O(24)–H(24)···O(16)#1[a]	0.879(18)	1.822(19)	2.6984(12)	174.6(17)
2	O(24)–H(24)···O(12A)	0.87(2)	1.81(2)	2.679(9)	174(2)
	O(24)–H(24)···O(12B)	0.87(2)	1.86(3)	2.719(16)	171(2)
	O(29)–H(29)···N(19)	0.88(2)	1.84(2)	2.7129(15)	172.2(19)
3 (Form I)	N(17)–H(17)···O(40)	1.01(2)	1.79(2)	2.792(2)	173(2)
	N(17)–H(17)···O(40)	0.90(2)	1.91(2)	2.806(2)	179(2)
	O(39)–H(39)···O(16)	1.02(3)	1.63(3)	2.618(2)	162(2)
	O(39)–H(39)···O(16)	1.01(3)	1.61(3)	2.602(2)	167(2)
	O(34)–H(34)···O(12)#1[b]	0.84(3)	1.88(3)	2.721(2)	178(2)
	O(34)–H(34)···O(12)#1[b]	0.99(3)	1.72(3)	2.707(2)	176(2)
4 (Form II)	O(29)–H(29)···O(16)	0.86(5)	1.76(5)	2.608(4)	168(5)
	N(17)–H(17)···O(30)	0.97(5)	1.75(5)	2.728(4)	178(4)
	O(24)–H(24)···N(19)#1[c]	0.77(6)	2.02(6)	2.748(4)	159(5)

[a] #1 $x + 2, y + 1, z$. [b] #1 $x - 1, y, z - 1$. [c] #1 $-x + 1/2, y - 1/2, -z + 1/2$.

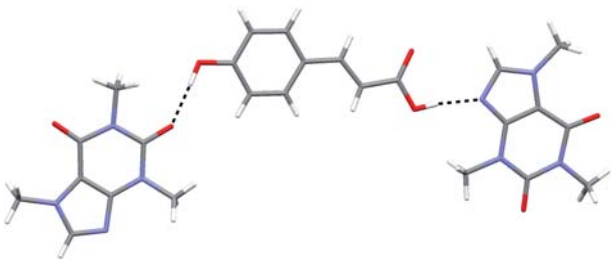

Fig. 3 Hydrogen bonding motifs between caffeine and *p*-coumaric acid in the discrete assembly **2**. The disorder and water molecule have been removed for clarity.

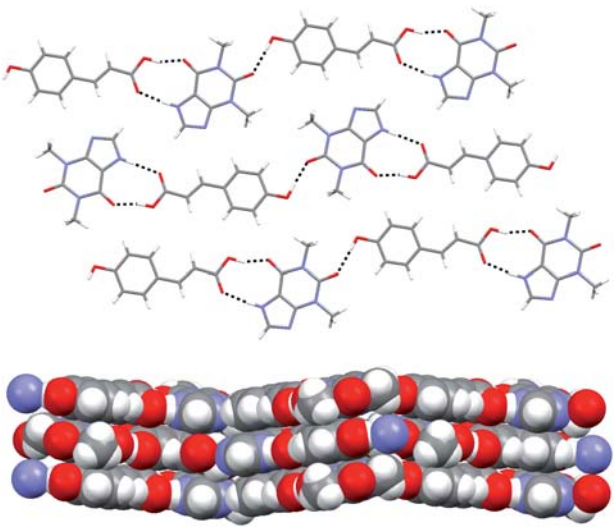

Fig. 4 Top view of the two-dimensional sheet composed of *p*-coumaric acid and theophylline **3** (Form I) (top) and side-view of the planar, stacked two-dimensional sheets (bottom).

two-dimensional sheets, Fig. 4. The 2-D sheets are stacked along the *a*-axis, into three dimensions, with distances as short as 3.30 Å between the layers.

The second 1 : 1 *p*-coumaric acid : theophylline cocrystal, **4** (Form II), crystallizes in the monoclinic space group $P2_1/n$ (Table 1). Within the asymmetric unit, one molecule of *p*-coumaric acid and one molecule of theophylline reside. Once again the same heteromeric synthon forms between the carboxylic acid moiety of *p*-coumaric acid and the imidazole proton and carbonyl moiety of theophylline (N17···O30, 2.728 Å, O29···O16, 2.608 Å). However, the hydroxyl moiety hydrogen bonds to the imidazole nitrogen atom (O24···N19, 2.748 Å) and not the carbonyl moiety of theophylline as displayed in **3** (Form I). The molecules assemble into one-dimensional, wave-like hydrogen-bonded chains, Fig. 5. Once again, the 2-D sheets are stacked along the *a*-axis, into three-dimensions, with distances as short as 3.40 Å between sheets.

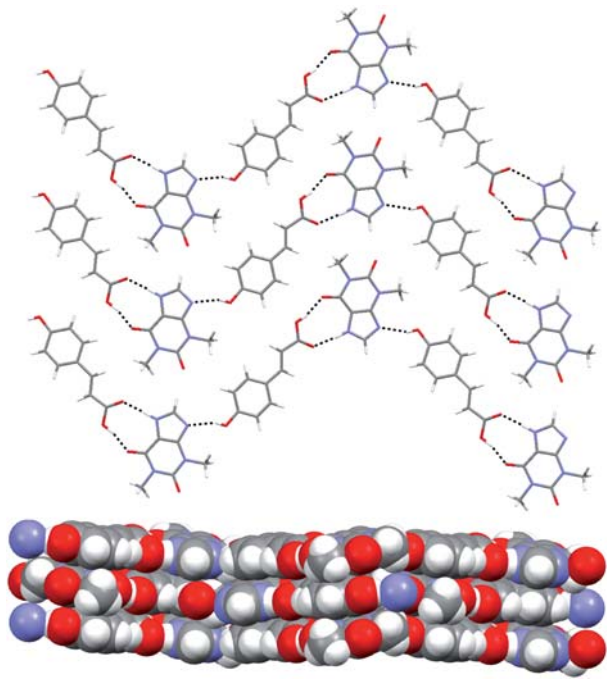

Fig. 5 Top view of the two-dimensional sheet composed of *p*-coumaric acid and theophylline **4** (Form II) (top) and side-view of the planar, stacked two-dimensional sheets (bottom).

By comparison, a 1 : 1 cocrystal between 4-hydroxybenzoic acid and theophylline has also been found, displaying the same hydrogen bonding patterns as seen in **4** (Form II), which includes acid–theophylline and hydroxyl–imidazole synthons.[19]

Polymorphism of single-component crystals is well documented and often occurs;[20] however, cases of cocrystal polymorphism have been reported much less frequently.[21] This is potentially due to the infancy of cocrystal screening and searching for polymorphs therein; not because it is less likely to occur. In fact, one could make the argument that it may even be more likely to occur, given the multifaceted nature of the typical coformers used for screening purposes.

Therefore, as for single-component systems, determining the thermodynamic relationship between polymorphs of cocrystals is important, especially throughout the drug development process, because changes in crystal form can lead to differences in physical and chemical properties.

Relative polymorph stabilities can usually be determined by experimental approaches. Typically, the onsets of melting and heats of fusion from differential scanning calorimetry (DSC) experiments can give some direction to the solid-form stability of polymorphic compounds;[20] however, cocrystals **3** and **4** decompose upon heating (see ESI†), and, thus, these parameters are unobtainable. Furthermore, the calculated densities from the single crystal structures are very close in value (**3**, Form I 1.483 g cm^{-3} and **4**, Form II 1.491 g cm^{-3}).[22] Additionally, both forms crystallized concomitantly upon slowly evaporating a 1 : 1 ratio of *p*-coumaric acid and theophylline, suggesting both forms are nearly identical in energy.[23] Nonetheless, equal amounts of each cocrystal (**3**, Form I and **4**, Form II) were slurried in saturated solutions of the individual components in three different solvents at ambient temperature. XRPD analysis on the remaining solids resulted in Form I, proposing it is the most stable form, of each sample, under these conditions. Along with the experimental results,[24] a computational modelling approach was also undertaken to examine the energy relationship between the polymorphs.

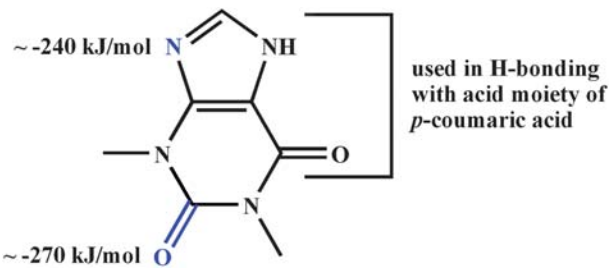

Scheme 2 Molecular structure of theophylline with calculated electrostatic charges for the imidazole N-atom and carbonyl moiety (both highlighted in blue).

The overall packing arrangement between forms is very similar, in which both form one-dimensional chains that result in relatively planar two-dimensional sheets. Not surprising, the two-dimensional sheets stack into three dimensions. From a hydrogen-bonding perspective, the major difference between the two forms resides primarily in the interactions of the hydroxyl moiety of *p*-coumaric acid. In **3**, Form I, the hydroxyl group hydrogen bonds to the carbonyl of theophylline, while in **4**, Form II, the hydrogen bond forms between the hydroxyl group and imidazole nitrogen atom. It has previously been shown that, based upon semi-empirical AM1 calculations, the highest point on the molecular electrostatic potential (MEP) surface can be utilized to estimate the propensity for forming electrostatic interactions (including hydrogen bonds).[25] Accordingly, this point for the imidazole N-atom on theophylline was found at about −240 kJ mol^{-1}, whereas for the carbonyl moiety it was found at about −270 kJ mol^{-1}. Thus, based on this method and following Etter's rules,[1a] the carbonyl oxygen would be slightly preferred over the imidazole nitrogen atom as the primary hydrogen bond acceptor (see Scheme 2).

The COMPASS calculations on the two polymorphic structures show a lattice energy difference of 1.32 kcal mol^{-1} per 1 : 1

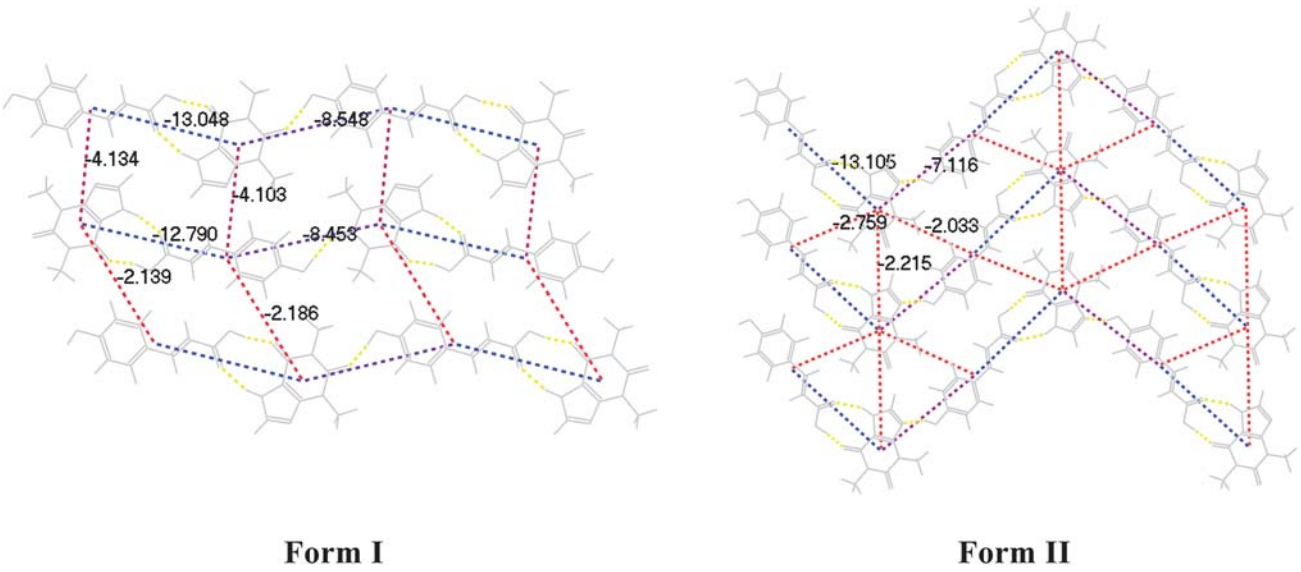

Fig. 6 Diagrams of the 1 : 1 *p*-coumaric acid : theopylline polymorphs displaying the interaction strength (kcal mol^{-1}) between molecules. Hydrogen bonds are represented as dashed-yellow lines and the strength of interaction follows dashed-lines: blue > purple > dark red > red.

stoichiometric unit of each cocrystal (**3**, Form I −232.09 kcal mol^{-1} and **4**, Form II −230.77 kcal mol^{-1}), favouring Form I as the more stable form. Force field calculations do not produce error bars, so the exact significance of this difference is unknown. Furthermore, it should be noted that the minimized structures represent the structures at minimal temperature, which excludes any consideration of entropy. Therefore, we cannot conclude with certainty, based on these calculations, which of the two forms is the most stable at room temperature; however, at the very least, the calculations show that the difference in enthalpy is very similar, which is consistent with our experimental results.

The computational studies sparked an interest in how the synthons and resulting three-dimensional structures differ between the two polymorphs. Fig. 6 shows the molecular interactions within the 2-D sheets. The strongest interactions (blue-dashed lines) are formed in both polymorphs by the hydrogen bonding pairs between the acid moiety of *p*-coumaric acid and theophylline. In Form II this interaction is −13.105 kcal mol^{-1}, whereas, due to the lower symmetry, two values were computed for Form I: −12.790 and −13.048 kcal mol^{-1}. A second set of interactions is found for the molecules interacting through a single hydrogen bond (purple-dashed lines). These are formed between the hydroxyl moiety of *p*-coumaric acid and either the carbonyl (−8.548 and −8.453 kcal mol^{-1}) or imidazole N-atom (−7.116 kcal mol^{-1}) of theophylline. These results correlate nicely to the MEP calculations, which also suggested the formation of the hydroxyl–carbonyl synthon (**3**, Form I) as energetically favoured over the hydroxyl–imidazole synthon (**4**, Form II). Weaker interactions (dark red to red-dashed lines) exist between the hydrogen bonded chains. Although the energies within the hydrogen bonded chains are quite similar between the two structures, the interactions between the chains are quite different. Form I shows an alternating pattern on one side of the chain of interactions as strong as −4.134 and −4.103 kcal mol^{-1}, whereas on the other side they are −2.139 and −2.186 kcal mol^{-1}. Form II shows a much more isotropic distribution of interactions between the chains, all being in the range −2.033 and −2.759 kcal mol^{-1} (Fig. 6). Each of the *p*-coumaric acid molecules forms two of these interactions, whereas the theophylline forms four, for a total of six interactions per stoichiometric, asymmetric unit in Form II. It is interesting that the total of six interactions adds up to −14.014 kcal mol^{-1}, whereas the total (four interactions) adds up to −12.562 kcal mol^{-1} in Form I.[26] Thus, what Form II lacks in hydrogen bonding energy, it mostly makes up for with its inter-chain interaction energies, where the total network energies add up to −27.701 kcal mol^{-1} for Form I and −27.228 kcal mol^{-1} for Form II.

Initially, it was believed that the inter-layer interaction energies would be quite uniform and similar between the two polymorphs, since the molecules possess the same surface area and, therefore, should roughly have the same van der Waals attraction. However, when the interaction energies are decomposed into molecular interactions, a much more intricate picture emerges. Fig. 7 shows the crystal graphs projected perpendicular to the layer orientation. In Form II the molecules interact mostly diagonally, producing a set of first order interactions in the range of −6.127 to −7.048 kcal mol^{-1}. A second order interaction is formed at −4.135 kcal mol^{-1} followed by a set of interactions in

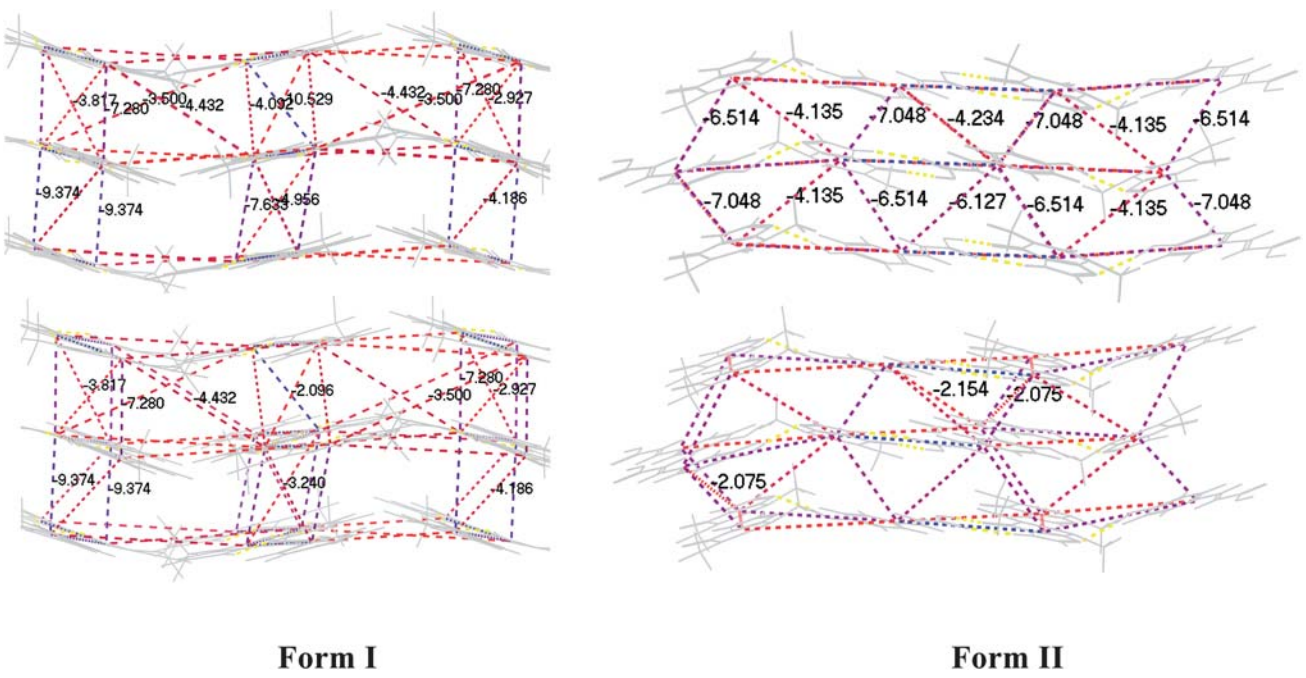

Fig. 7 Diagrams of the 1 : 1 *p*-coumaric acid : theopylline polymorphs displaying the inter-layer interaction energies (kcal mol^{-1}) between molecules. All the crystal graph interactions are shown, but, for clarity, only the inter-layer interactions are labelled. The top view is a perpendicular projection with respect to the layers. For Form I, the structure is projected along the periodic hydrogen bonded chains. The strongest inter-layer interactions show up in pairs because of how the chains cross into the plane of projection, which is shown more clearly in the slightly tilted bottom view projection. For Form II some weaker bonds in the order of −2 kcal mol^{-1} are obscured in the top projection due to how the interactions zigzag along the projection vector. The bottom view is slightly tilted to reveal those interactions (red lines, only labelled in the bottom view).

the range of −2.075 to −2.154 kcal mol^{-1}. Please note that an arbitrary cut-off of −2 kcal mol^{-1} was applied for the interactions considered for this discussion and that many interactions exist below this level of energy. Form I shows a number of interactions that are much stronger between the layers than those found in Form II, −9.374 and even −10.529 kcal mol^{-1}. This is due to a larger spatial overlap; the interactions thereby align in a more vertical orientation. Every molecule interacts with each layer beneath and above it with at least −7.280 kcal mol^{-1}. This shows that the energies of the interactions between the layers are comparable to those of hydrogen bonds. An in-depth analysis of these interactions revealed that they are mostly dominated by the van der Waals attraction, where the strongest interactions lower their energy by having atoms of opposite partial charge in close proximity (see ESI† for a more detailed explanation). In addition to these van der Waals interactions, Form I forms more diagonally oriented interactions that quickly dwindle to lower and lower interaction strengths. Interestingly, the initial description of cocrystals **3** and **4**, as structures of 2-D sheets that stack to form into a 3-D crystal is significantly changed. The stacking interactions by far outweigh the lateral interactions between the hydrogen bonded chains.

It is instructive to see how these polymorphs distribute their interaction energies and what constitutes the structural driving forces (hydrogen bonding, van der Waals forces,…), to ultimately assess the relative stabilities of the two forms. All in all, it is the total (free) lattice energy that decides which form is most stable at a given set of environmental conditions. In the case of the *p*-coumaric acid : theophylline cocrystals, Form I (cocrystal **3**) appears most stable at low temperature, based on the computational analysis performed.

This kind of exercise also affords information regarding how the crystals may behave physically. In general, a more isotropic distribution of energies, for instance, leads to a more isotropic crystal morphology, which can be beneficial (due to better flowability and filterability) when processing these materials. The existence of planes of low energy within the structure observed in Form I can lead to low shear strength which influences plastic *versus* brittle behaviour, in turn affecting the processing behaviour and drug product quality such as compactibility, friability, and compressibility. When the total lattice energies are sufficiently close, as is indicated both by our experimental and computational efforts, these properties may lead to a decisive factor in solid form selection for single component or multi-component product applications.

Conclusions

We have successfully shown that the nutraceutical compound *p*-coumaric acid does cocrystallize with caffeine and theophylline, resulting in four cocrystalline materials. Single crystal structures were determined for each cocrystal, which allowed for a better understanding of the hydrogen bonding interactions, especially between the two 1 : 1 *p*-coumaric acid : theophylline polymorphs.

Determining the relative stability of the 1 : 1 *p*-coumaric acid : theophylline cocrystal polymorphs proved very difficult at room temperature. Both the experimental and computational methods suggest that the difference in energy is very small. The computational analyses suggest that Form I is favoured as the low temperature form, albeit by a small difference in enthalpy, while slurry interconversion experiments show Form I as the most stable at room temperature. We have shown in great detail that the crystal graphs of Forms I and II are distinctly different. This full decomposition of the lattice energy can be a great asset in the evaluation of how the molecules are actually interacting in the crystal structure, which is an extremely useful tool in the design of cocrystals and their resulting materials properties. We have shown that the application of cocrystals is viable, at least for these systems, and that polymorphism of these systems may lead to opportunities in form selection to optimize the performance of these crystals.

Acknowledgements

We would like to thank Dr John Desper (Kansas State University) for single-crystal data collection and structure solution of **1**–**4** and SSCI's analytical services for data collection. We also thank Mr Eyal Barash, Dr Sarah Bethune, and Dr Brett Cowans for their careful review of this manuscript.

Notes and references

1 (*a*) M. C. Etter, *Acc. Chem. Res.*, 1990, **23**, 120–126; (*b*) C. B. Aakeroy and D. J. Salmon, *CrystEngComm*, 2005, **7**, 439–448; (*c*) L. MacGillivray, *CrystEngComm*, 2004, **6**, 77–78; (*d*) G. R. Desiraju, *Acc. Chem. Res.*, 2002, **35**, 565–573; (*e*) B. Moulton and M. Zaworotko, *Chem. Rev.*, 2001, **101**, 1629–1658; (*f*) J.-M. Lehn, *Science*, 2002, **295**, 2400–2403; (*g*) F. Grepioni and D. Braga, *Making Crystals by Design—from Molecules to Molecular Materials, Methods, Techniques, Applications*, Wiley-VCH, Weinheim, Germany, 2007, ch. 2.5 and references therein.

2 (*a*) A. V. Trask, W. D. S. Motherwell and W. Jones, *Cryst. Growth Des.*, 2005, **5**, 1013–1021; (*b*) A. V. Trask, W. D. S. Motherwell and W. Jones, *Int. J. Pharm.*, 2006, **320**, 114–123; (*c*) D. J. Good and N. Rodríguez-Hornedo, *Cryst. Growth Des.*, 2009, **9**, 2252–2264; (*d*) S. L. Childs, N. Rodríguez-Hornedo, L. S. Reddy, A. Jayasankar, C. Maheshwari, L. McCausland, R. Shipplett and B. C. Stahly, *CrystEngComm*, 2008, **10**, 856–864; (*e*) M. B. Hickey, M. L. Peterson, L. A. Scoppettuolo, S. L. Morisette, A. Vetter, H. Guzman, J. F. Remenar, Z. Zhang, M. D. Tawa, S. Haley, M. J. Zaworotko and Ö. Almarsson, *Eur. J. Pharm. Biopharm.*, 2007, **67**, 112–119; (*f*) D. McNamara, S. L. Childs, J. Giordano, A. Iarriccio, J. Cassidy, M. S. Shet, R. Mannion, E. O'Donnell and A. Park, *Pharmacol. Res.*, 2006, **23**, 1888–1897; (*g*) N. Schultheiss and A. Newman, *Cryst. Growth Des.*, 2009, **9**, 2950–2967 and references therein; (*h*) N. Blagden, M. De Matas, P. T. Gavan and P. York, *Adv. Drug Delivery Rev.*, 2007, **59**, 617–630; (*i*) S. L. Childs, L. J. Chyall, J. T. Dunlap, V. N. Smolenskaya, B. C. Stahly and G. P. Stahly, *J. Am. Chem. Soc.*, 2004, **126**, 13335–13342; (*j*) K. Shiraki, N. Takata, R. Takano, Y. Hayashi and K. Terada, *Pharmacol. Res.*, 2008, **25**, 2581–2592; (*k*) T. Friščić and W. Jones, *Cryst. Growth Des.*, 2009, **9**, 1621–1637; (*l*) P. Vishweshwar, J. A. McMahon, J. A. Bis and M. J. Zaworotko, *J. Pharm. Sci.*, 2006, **95**, 499–516; (*m*) Ö. Almarsson and M. J. Zaworotko, *Chem. Commun.*, 2004, 1889–1896; (*n*) W. Jones, W. D. Samuel Motherwell and A. V. Trask, *MRS Bull.*,2006, 31, 875–879; (*o*) *Crystal growth and Design 'virtual issue' on cocrystals*, http://pubs.acs.org/page/cgdefu/vi/1.

3 *Handbook of Pharmaceutical Salts: Properties, Selection and Use*, ed. P. H. Stahl and C. G. Wermuth, Verlag Helvetica Chimica Acta, Zürich, 2002.

4 *Generally Regarded as Safe*, http://www.cfsan.fda.gov/~rdb/opa-gras.html and http://www.cfsan.fda.gov/~dms/grasguid.html.

5 *Everything Added to Food Stuff in the United States*, http://vm.cfsan.fda.gov/~dms/eafus.html.

6 *Handbookof Pharmaceutical Excipients*, ed. R. C. Rowe, P. J. Sheskey, and S. C. Owen, APhA Publications, 5th edn, 2005.

7 A 'nutraceutical compound' can be defined as 'a food (or part of a food) that provides medical or health benefits, including the prevention and/or treatment of a disease and possesses a physiological benefit or reduces the risk of chronic disease', E. K. Kalra, *AAPS PharmSci.*, 2003, **3**, article 25, pp. 1–2.
8 A few combination formulations; Berodual (fenoterol and ipratropium); Kaletra (Ritonavir and Lipinavir); Advair (Fluticasone and Salmeterol); Epzicom (Abacavir and Lamivudine).
9 (*a*) S. T. Talcott, C. E. Duncan, D. D. Pazo-Insfran and D. W. Gorbet, *Food Chem.*, 2005, **89**, 77–84; (*b*) M. P. Kähkönen, A. I. Hopia, H. J. Vuorela, J. P. Rauha, K. Pihlaja, T. S. Kujala and M. Heinonen, *J. Agric. Food Chem.*, 1999, **47**, 3954–3962.
10 L. R. Ferguson, Z. Shou-tun and P. J. Harris, *Mol. Nutr. Food Res.*, 2005, **49**, 585–693.
11 (*a*) C. Luceri, L. Giannini, M. Lodovici, E. Antonucci, R. Abbate, E. Masini and P. Dolara, *Br. J. Nutr.*, 2007, **97**, 458–463; (*b*) F. Guglielmi, C. Luceri, L. Giovannelli, P. Dolara and M. Lodovici, *Br. J. Nutr.*, 2003, **89**, 581–587; (*c*) C. Luceri, F. Guglielmi, F. Meoni and P. Dolara, *Scand. J. Gastroenterol.*, 2004, **39**, 1128–1133.
12 http://www.medicinenet.com/theophylline/article.htm.
13 *APEXII v. 2009.11–0, © 2005–2009*, Bruker Analytical X-ray Systems, Madison, WI.
14 *SAINT v7.68A, © 1997–2009*, Bruker Analytical X-ray Systems, Madison, WI.
15 *SHELXTL v. 2008/4, © 2008*, Bruker Analytical X-ray Systems, Madison, WI.
16 (*a*) H. Sun, *J. Phys. Chem. B*, 1998, **102**, 7338–7364; (*b*) H. Sun, P. Ren and J. R. Fried, *Comput. Theor. Polym. Sci.*, 1998, **8**, 229–246; (*c*) D. Rigby, H. Sun and B. E. Eichinger, *Polym. Int.*, 1997, **44**, 311–330.
17 Pictures created using Mercury CSD 2.2.
18 D.- K. Bučar, R. F. Henry, X. Lou, R. W. Duerst, L. R. MacGillivray and G. G. Z. Zhang, *Cryst. Growth Des.*, 2009, **9**, 1932–1943.
19 S. L. Childs, G. P. Stahly and A. Park, *Mol. Pharmacol.*, 2006, **3**, 328–338.
20 (*a*) S. R. Byrn, R. R. Pfeiffer and J. G. Stowell, *Solid-State Chemistry of Drugs*, SSCI, Inc., West Lafayette, 2nd edn, 1999; (*b*) H. Brittain, *Polymorphism in Pharmaceutical Solids*, Marcel Dekker, New York, 1999; (*c*) J. Bernstein, *Polymorphism in Molecular Crystals*, Clarendon, Oxford, 2002; (*d*) R. Hilfiker, *Polymorphism: in the Pharmaceutical Industry*, Wiley-VCH, New York, 2006; (*e*) G. P. Stahly, *Cryst. Growth Des.*, 2007, **7**, 1007–1026.
21 (*a*) S. Aitipamula, P. S. Chow and R. B. H. Tan, *CrystEngComm*, 2009, **11**, 889–895; (*b*) S. Aitipamula, P. S. Chow and R. B. H. Tan, *CrystEngComm*, 2009, **11**, 1823–1827; (*c*) N. J. Badu, L. S. Reddy, S. Aitipamula and A. Nangia, *Chem.–Asian J.*, 2008, **3**, 1122–1133; (*d*) D. Braga, G. Palladino, M. Polito, K. Rubini, F. Grepioni, M. R. Chierotti and R. Gobetto, *Chem.–Eur. J.*, 2008, **14**, 10149–10159; (*e*) A. N. Sokolov, D. L. Swenson and L. R. MacGillivray, *Proc. Natl. Acad. Sci. U. S. A.*, 2008, **105**, 1794–1797.
22 The difference in calculated crystal density is less than 1% between polymorphic forms. It has been noted that differences less than 1% should be excluded from the density rule (ref. 20*c*, p. 41).
23 J. Bernstein, R. J. Davey and J.-O. Henck, *Angew. Chem., Int. Ed.*, 1999, **38**, 3440–3461.
24 Solution calorimetry (to determine heats of solution) and/or hyper-DSC (to obtain heat of fusion values) could have also been introduced to aid in determining thermodynamic stabilities.
25 (*a*) C. A. Hunter, *Angew. Chem., Int. Ed.*, 2004, **43**, 5310–5324; (*b*) M. Kamieth, F.-G. Klärner and F. Diederich, *Angew. Chem., Int. Ed.*, 1998, **37**, 3303–3305; (*c*) C. B. Aakeröy, M. Fasulo, N. Schultheiss, J. Desper and C. Moore, *J. Am. Chem. Soc.*, 2007, **129**, 13772–13773; (*d*) C. B. Aakeröy, D. J. Salmon, M. M. Smith and J. Desper, *Cryst. Growth Des.*, 2006, **6**, 1033–1042; (*e*) N. Schultheiss, K. Lorimer, S. Wolfe and J. Desper, *CrystEngComm*, 2010, **12**, 742–749.
26 Notice that the numbers need to be divided by two when calculating the energies as a portion of the lattice energy due to double counting of interactions.